ORIGINAL PAPER

Improvement of dye-sensitized solar cell performance through electrodepositing a close-packed TiO$_2$ film

Min Wu · Z. H. Yang · Y. H. Jiang · J. J. Zhang ·
S. Q. Liu · Y. M. Sun

Abstract A simple electrodepositing method was proposed for fabricating a uniform, tight, and close-packed TiO$_2$ nanocrystalline film on the ITO substrate. The electrode and dye-sensitized solar cell (DSSC) with electrodeposited TiO$_2$ layer were characterized by scanning electron microscopy, cyclic voltammetry, and electrochemical impedance spectroscopy. The phthalocyanin dye, zinc tetra-carboxyl phthalocyanin complex, was used as a model dye to evaluate the influence of close-packed TiO$_2$ blocking layer on the photocurrent–voltage property. On the electrodeposition, the close-packed TiO$_2$ layer could effectively inhibit the recombination of charges, and therefore improve the performances of the corresponding cells. The effects of film thickness on light transmittance and photocurrent density of the corresponding cell were also demonstrated. The optimum film thickness was found to be approximately 400 nm. At the optimum thickness, the photocurrent density greatly increased comparing with that of the screen printing TiO$_2$ film. These results imply that our proposition was a potential and feasible method for the fabrication of DSSC practically.

Keywords TiO$_2$ nanocrystalline film · Electrodeposition · Photocurrent · Electrochemical impedance spectroscopy · Zinc tetra-carboxyl phthalocyanin complex

M. Wu (✉) · Y. H. Jiang · J. J. Zhang · S. Q. Liu · Y. M. Sun
School of Chemistry and Chemical Engineering,
Southeast University,
Nanjing 211189, China
e-mail: wuminnj@163.com

Z. H. Yang
Xin Anjiang Vocation School,
Hangzhou 311600, China

Introduction

Recently, dye-sensitized solar cell (DSSC), a device that converts sunlight into electricity on the base of dye-sensitized TiO$_2$ nanocrystalline film, has attracted considerable attention due to its low cost, widely available and biocompatible material, and wide band gap [1, 2]. In a DSSC, an electron transfer cycle was completed by the following process, i.e., the light induced electron rendered into the conducting band of TiO$_2$ nanocrystallite, and the oxidized dye was reduced in electrolyte by redox couples, usually as iodide/triiodide (I$^-$/I$_3^-$). It was reported that the efficiency of photogenerated electron transition could be improved by using TiO$_2$ nanocrystallites [1, 3, 4]. A network and transparent mesoporous structure formed by TiO$_2$ nanocrystallites were ideal for dye loading, thus the sufficient light absorption was benefited. Even though, how to decrease the back reaction of photo-injected electrons with I$_3^-$ was still a challenge.

The opened three-dimensional mesoporous TiO$_2$ film should favor the electrolyte to penetrate the film to the back contact and induce the dark current at the boundary of conductive substrate. Hence, for enhancement of the DSSC efficiency, it was essential to avoid the recapture of photo-injected electrons by I$_3^-$, thereby to prevent charges from recombination. Previous investigations demonstrated that it was effective to introduce a compact and thin layer of TiO$_2$ underlayer onto the transparent conducting glass substrate, which resulted in the decrease of dark current and enhancement of the DSSC efficiency [5–10]. Three methods were applicable for fabricating such compact TiO$_2$ film, namely spray pyrolysis [5, 7], electrophoretical deposition [6], and dip coating [9]. Spray pyrolysis deposits a compact TiO$_2$ underlayer followed by coating a meso-porous TiO$_2$ layer with screen printing [5, 7]. Grätzel and

co-workers [7] invented it for the suppression of dark current so as to increase V_{OC}. Peng [8] obtained a compact TiO_2 layer with the best photovoltaic properties at an optimum film thickness of 150 nm corresponding to ten cycles spraying by using an aerosol of titanium (IV) bis (acetoacetonato) di(isopropanoxylate) (TAA) in ethanol as the spraying substrate. However, the disadvantages of spray pyrolysis were obvious. For example, high temperature was essential to pyrolyze the organic substance into gas state; in addition, multi-step and time-costing operation with more than ten spraying cycles was also disadvantageous. Yum et al. [6] developed the electrophoretical deposition. They reported that the current density was increased obviously, with its low cost, relatively fast and reproducible, whereas the improvement in interconnection between nanocrystalline TiO_2 by compression was needed. Hart et al. [9] declared that a compact film of TiO_2 sol–gel blocking layer was constructed by dip-coating method. It increased the short-circuit current, but the operation was complicated and the thickness of film was uncontrollable. Anyway, these studies illustrated that the dark current charge recombination occurred mainly near the conductive substrate and not across the entire TiO_2 film; thus, the formation of TiO_2 underlayer on a conductive substrate could effectively block the dark current.

In the present work, which targeted to overcome all those demerits of the above methods, an electrodepositing method was developed for preventing the loss of photo-injected electrons from the back reaction in DSSC solar cell. It was simple and economic, compared with the above methods.

Experimental

Materials

$TiCl_3$ was obtained from Sigma Aldrich Co. Ltd. (USA). Tetrabutylorthotitanate ($C_{16}H_{36}O_4Ti$) was purchased from Lingfeng Chemical Co. Ltd. (Shanghai, China). Tetrabuty-lammonium perchlorate ($C_{16}H_{36}NClO_4$, TBAP) was obtained from Xianju Medicine and Chemical Co. Ltd. (Zhejiang, China). The colloidal TiO_2 solution for screen printing was prepared by dropwise adding (one drop per 5 s) a mixture of 12.5 ml tetrabutylorthotitanate and 4 ml isopropanol into 150 ml H_2O containing 2 ml dense HNO_3. The solution was then kept at 75 °C for 5 h after adding PEG800 into the solution so as to avoid the aggregation of TiO_2 particles. TiO_2 colloid was thus obtained and stored at room tempeture for the following use.

Zinc tetra-carboxyl phthalocyanin complex was synthe-sized according to the reference [11] with slight modifica-tion as shown in Scheme 1. Briefly, mixing 6.8 g trimellitic anhydride, 2.2 g zinc acetate, and 12.0 g urea at first and then adding 0.02 g ammonium molybdate as catalyst, the mixture was heated to 200 °C for the high yield of intermediate. Thereafter, it was refluxed in potassium hydroxide for 20 h at 100 °C and washed with 2.0 M hydrochloric acid for several times. The yield of ZnTCPc was ca. 1.02 g.

The resistance of ITO conductive glass was 15 Ω/sq. All other chemicals were of analytical grade and used without further purification.

### Systhesis of TiO_2 close-packed layer on ITO electrodes

Prior to each electrodeposition, the ITO glass was cleaned by soaking in $KOCH(CH_3)_2$ for 0.5 h to erase the grease. Thereafter, it was ultrasonicated thoroughly with distilled water and ethanol, respectively, and then dried with nitrogen flow.

For preparation of the close-packed TiO_2 layer on ITO electrode surface, the electrolyte was prepared by diluting 8 ml 20–30 wt.% $TiCl_3$ solution with deoxygenated deionized water to 40 ml and adding 0.1 g of Zn powder in order to prevent Ti^{3+} from the oxidation to Ti^{4+}, and then kept in dark for 12 h. After adjusting pH to 2.2–2.5 by the saturated NaOH aqueous solution, the electrodeposition was performed, using a conventional three-electrode elec-trochemical cell equipped with a Pt-wire auxiliary elec-trode, a saturated calomel electrode (SCE) reference electrode, and an ITO conductive glass (1×2 cm^2) as the working electrode at 0.1 V during different time periods. After washing thoroughly with deionized water and dried under infrared lamp, the resulting TiO_2 electrodeposited electrodes, denoted as $eTiO_2$/ITO, was used for further coating a layer of TiO_2 film (about 5 μm thickness) by screen printing method. After being annealed at 450 °C for 30 min under ambient conditions, the electrodes with two-layer TiO_2 film ($tTiO_2$/ITO) were thus obtained. For comparison, the mono-screen-printing electrode ($sTiO_2$/ITO) without TiO_2 electrodeposited layer was prepared only by screen printing followed by annealing at 450 °C for 30 min under ambient conditions. All the results are reproducible.

The morphologies of the nanocrystalline TiO_2 film electrodes were characterized by scanning electron micros-copy (SEM, LEO 1530 VP, Germany). Gold was used as the sputtering material.

Zinc tetra-carboxyl phthalocyanine-sensitized TiO_2 film

Piror to sensitization, TiO_2 particles was pretreated by immersing TiO_2 film-coated electrodes into pH 3.0 HCl solution for 12 h. The electrode was washed thoroughly

Scheme 1 The synthesis of zinc tetra-carboxyl phthaocyanine (ZnPcTc)
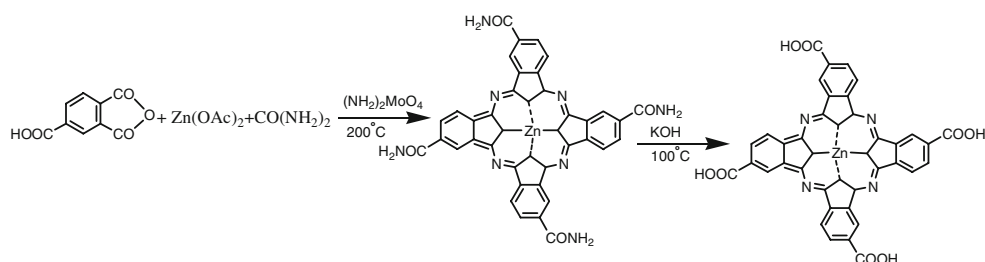
with water and dried at atmosphere. After heating at 120 °C for 2 h, the electrode was soaked in 0.5 mM DMF solution of ZnTCPc for 24 h. It was then rinsed thoroughly with DMF and dried at 120 °C for 2 h to form a dye-sensitive TiO_2 film electrode.

Measurements

The UV–vis transmittance spectra of TiO_2 film electrode were performed with a UV-2201 spectrophotometer (Hitachi Shimadzu, Japan). Electrochemical measurements were carried out with a CHI 750C electrochemical station. Cyclic voltammetric experiments and electrochemical impedance spectroscopy were recorded by using a three-electrode system, a nanocrystalline TiO_2 film working electrode (geometric area of 25 mm^2), a platinum auxiliary electrode, and a saturated sodium calomel electrode (SCE) reference electrode. The electrolyte was 2.5 mM 1:1 $K_4Fe(CN)_6$/$K_3Fe(CN)_6$ in 0.1 M KCl solution. All experimental solutions were deoxygenated by bubbling highly pure nitrogen for 30 min, and maintained under nitrogen atmosphere during measurements.

Photocurrent–voltage characteristics of dye-sensitized TiO_2 film electrodes were measured with sandwich-type cells. Dye-sensitized TiO_2 film was used as a working electrode, while Pt sputtered on ITO was used as a counter electrode. The electrolyte was 0.5 M KI+0.05 M I_2 in propylene carbonate. Photocurrent–photovoltage characteristics of solar cells were measured by a Keithley model 2400 digital source meter using a NEWPORT Oriel 91192 solar simulator (NEWPORT, USA) equipped with AM 1.5 filter and the intensity was adjusted to 100 mW/cm^2.

**Results and discussion**

The preparation of TiO_2 film

It has been reported that the formation of TiO_2 underlayer on a conductive substrate could effectively block dark current, and thus being widely used in DSSC design [5–10]. In the present work, a close-packed eTiO_2/ITO prepared by electrodeposition was applied. For comparison, sTiO_2/ITO was also constructed. Figure 1 showed the SEM

images of top-view TiO_2 layer on ITO substrate fabricated by electrodeposition at 0.1 V for 20 min (a) and by screen printing method (b). The average particle size estimated from the SEM image was about 20 nm (Fig. 1a), whereas it was approximately 30 nm by screen printing methods (Fig. 1b). Meanwhile, as shown in Fig. 1a, the electrodeposited TiO_2 layer had a densely packed and homogeneous structure, whilst porous morphology was observed for sTiO_2/ITO. It indicated that a compact layer of TiO_2 film on ITO substrate was achieved by electrodeposition.

Furthermore, the film thicknesses of close-packed TiO_2 on ITO electrode surface were determined by SEM. The close-packed TiO_2 layers were deposited in 20–30 wt.% $TiCl_3$ solution at 0.1 V for (a) 15, (b) 25, and (c) 35 min, respectively. As shown in Fig. 2, after electrodepositing for 15 min, a flat and compact layer of TiO_2 film with thickness of 200 nm was grown on the top of ITO surface. The film thickness increased with the increase of electrodeposition time (Fig. 2b, c). For example, as the depositing time was prolonged from 25 to 35 min, it increased from 320 to 460 nm. However, it should be noted that the heterogeneously distributing film due to the layer stack of TiO_2 nanoparticles was observed when the depositing time was 35 min (not shown), and further studies showed that the performance of solar cells with such heterogeneous TiO_2 film was poor. Therefore, it was concluded that the film thickness should be controlled at less than 400 nm, and that the depositing time should be around 25 min. Hereby, a flat and compact TiO_2 film with a film thickness of approximately 400 nm was achieved. This film, applied for the following studies, was expected to prevent the electrolyte from diffusing through the film to reach the back contact of conductive substrate and in turn to reduce the recombination of charges.

The formation of close-packed TiO_2 film on the surface of ITO by electrodepositing was also evidenced by electrochemical results. The redox couple $Fe(CN)_6^{3-/4-}$ was widely used as an electrochemical probe in the electrochemical study, especially for the characterization of film-modified electrodes. Using $K_3[Fe(CN)_6]$/$K_4[Fe(CN)_6]$ as probe, as shown in Fig. 3a, it displayed a pair of well-defined redox peaks of $Fe(CN)_6^{3-/4-}$. After a compact TiO_2 layer was coated, poor redox peaks with a peak-to-peak separation potential of 565 mV were observed

Fig. 1 The SEM images of a top-view TiO$_2$ layer on ITO fabricated by **a** electrodeposition at 0.1 V for 20 min, **b** by screen printing method
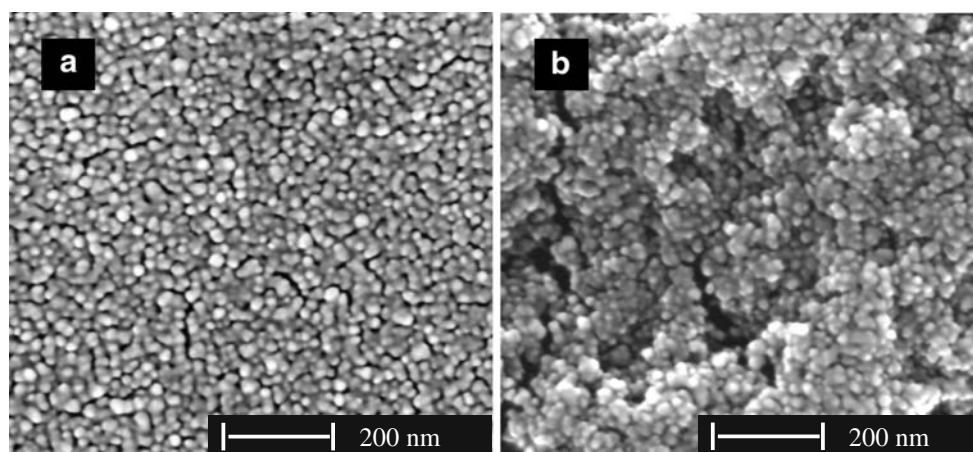
for eTiO$_2$/ITO (Fig. 3b). Moreover, the peak currents of sTiO$_2$/ITO showed slight decrease, comparing with those of bare ITO electrode (Fig. 3c). These results indicated that, as expected, the close-packed TiO$_2$ nanocrystalline film on ITO effectively blocked the electron transfer from ferricyanide to the electrode. Additionally, it prevented ferricyanide from penetrating the film, thereby blocking the exchange of electron with electrode. As a result, it decreased the electrochemical response of electroactive probe.

The results of electrochemical impedance spectra further supported the formation of densely packed TiO$_2$ layer by electrodeposition. As we know, impedance spectroscopy was an effective approach to probe the interfacial properties of surface-modified electrode [12–17]. The complex impedance was donated as the real, Z_{re}, and imaginary, Z_{im}, components mainly originating from the resistance and capacitance of cell, respectively. Figure 4a showed the AC impedance spectra for (a) bare ITO substrate, (b) electrodeposition, (c) screen printing, and (d) electrodeposition following screen printing TiO$_2$ film electrode in 0.1 M KCl solution containing 2.5 mM Fe(CN)$_6^{3-/4-}$ at an open circumpotential. An equivalent circuit $R_s(R_{ct}CPE)W_o$ (Fig. 4b) was used to model the impedance data, thus enabling the extraction of electrical parameters, such as resistance, from the impedance spectra [18]. In this circuit, R_s represented the ohmic resistance of electrolyte, while the parallel combination of charge-transfer resistance (R_{ct}) appeared when a redox probe existed in the electrolyte solution and the constant phase element (CPE) led to a depressed semicircle in the corresponding Nyquist impedance plot, and W_o was the Warburg impedance resulted from the diffusion of ions from the bulk electrolyte to electrode. CPE was defined by CPE-T and CPE-P. If CPE-P was 1, then CPE was considered as a capacitor C_{dl}. The components R_s and W_o in the electronic circuit represented bulk properties of electrolyte solution and diffusion features of redox probe in solution. The other two components in

circuit, CPE and R_{ct}, represented the interfacial properties of electrode and they were affected by coating the nanostructured materials onto the electrode surface. Therefore, the analysis of CPE and R_{ct} could give important information of the varying extent of surface properties.

It was expected to introduce a barrier for the electron transfer at the electrode interface by coating TiO$_2$ film on the electrode surface. As a result, an enhanced electron transfer resistance (R_{ct}) was observed from 171.4 Ω for the bare ITO electrode to 476.0 Ω for sTiO$_2$/ITO and 591.4 Ω for eTiO$_2$/ITO, respectively. The reason for the increase in R_{ct} for eTiO$_2$/ITO relative to sTiO$_2$/ITO was considered that the denser packed TiO$_2$ nanoparticles on the electrode surface stopped the ferricyanide from exchanging electron with electrode, thereby effectively blocking the reactions of redox active species at electrode. R_{ct} of eTiO$_2$/ITO further increased from 591.4 to 812.1 Ω by coating a mesoporous layer on the electrodeposited TiO$_2$ film. It possibly resulted from the accumulative effect of impedance at both electrodepositing and screen printing TiO$_2$ layer. Hence, the introduction of densely packed TiO$_2$ layer between ITO substrate and mesoporous TiO$_2$ layer enhanced the power conversion efficiency of DSSC by preventing the electrolyte from bypassing the film and reducing charge recombination at the boundary of conductive substrate.

## The effect of film thickness on light transmittance and photocurrent

The close-packed TiO$_2$ film was transparent, which transmitted more than 90% of injected lights. Figure 5 showed spectra of UV–vis transmittance of TiO$_2$ film electrode prepared by electrodeposition at 0.1 V for 20 min referencing a bare ITO. The transmittance of deposited TiO$_2$ film increased with the red shift of wavelength and leveled off in the range of wavelength longer than 581 nm. The largest transmittance considerably favored phthalocyanine dyes of TCZnPc to gain the highest absorbance of Q
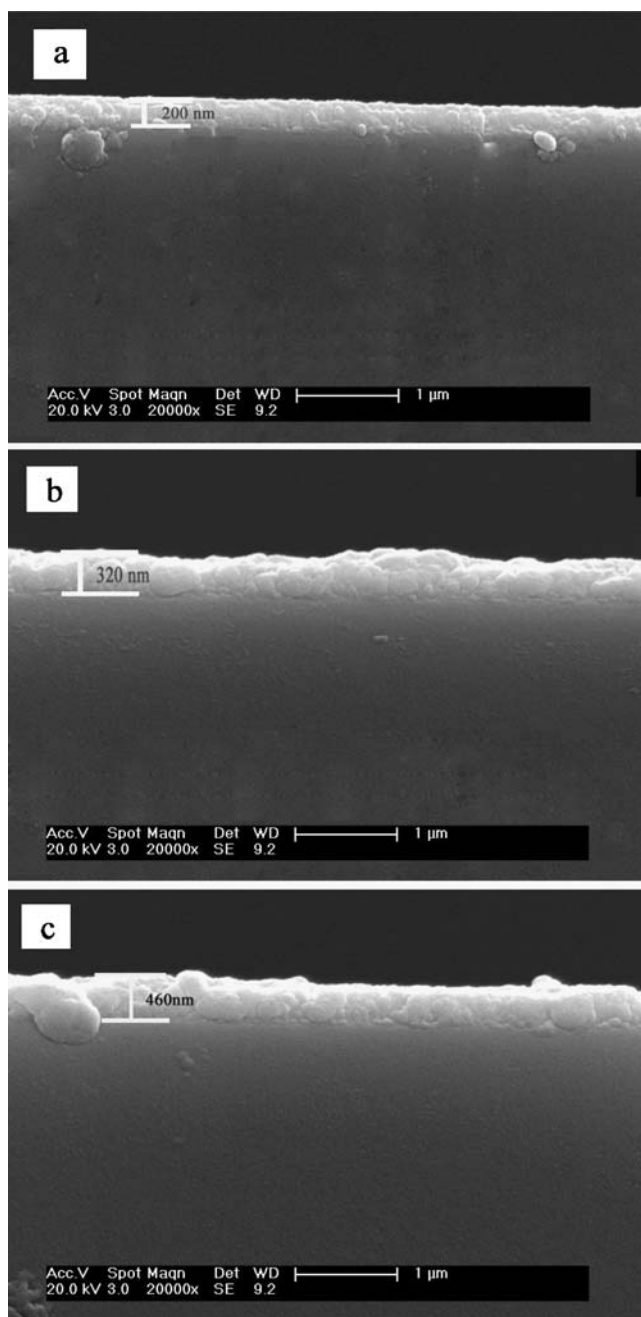
Fig. 2 Cross-section SEM images of the close-packed TiO_2 layers prepared by electrodepositing at 0.1 V for **a** 15, **b** 25, and **c** 35 min

band between 600 and 800 nm, thus the high energy conversion efficiency was expectable.

The light transmittance of $eTiO_2/ITO$ was dependent to the thickness of electrodepositing TiO_2 film. By varying the depositing time, a series of samples with increased thickness was obtained. It was observed that the transmittance of various films at 358 nm decreased from 96% to 20% as the depositing time prolonged (Fig. 6). Moreover, the thickness can be readily controlled by changing deposition parameters such as deposition time.
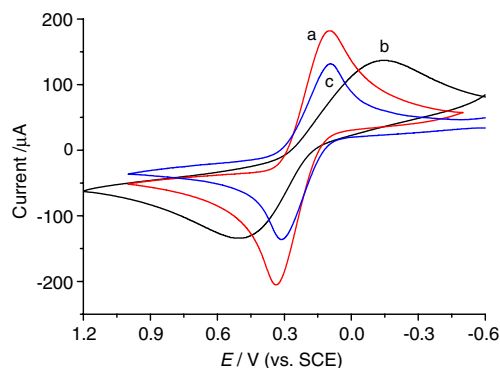

Fig. 3 Cyclic voltammograms of **a** bare ITO substrate, **b** electrodeposition, and **c** screen printing TiO_2 film electrode in 0.1 M KCl solution containing 2.5 mM $K_4Fe(CN)_6$/$K_3Fe(CN)_6$

Further investigation was carried out by screen printing a mesoporous TiO_2 layer on the above $eTiO_2/ITO$. Accordingly, the $tTiO_2/ITO$ with different thickness of close-packed TiO_2 underlayer was prepared. After being annealed and immersed in HCl solution, the $tTiO_2/ITO$ was soaked in 0.5 mM ZnTCPc for 24 h to obtain dye-sensitized TiO_2 film electrodes. Equipped with a dye-sensitized TiO_2 film electrode as working electrode, ITO sputtered by Pt as counter electrode, sandwich cells were employed to evaluate the photocurrent–voltage performances of dye-sensitized TiO_2 film electrodes. Figure 5 displayed the plots of related photocurrent density versus film thickness. The
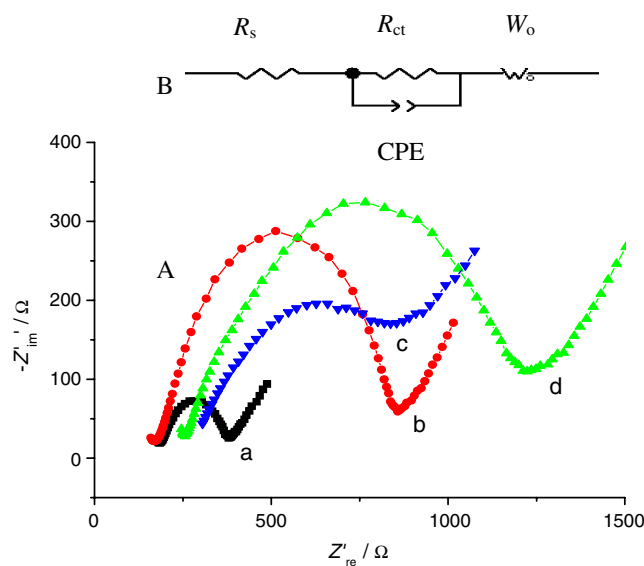
Fig. 4 **a** Nyquist plots of (*a*) bare ITO substrate, (*b*) electrodeposition, (*c*) screen printing, and (*d*) electrodeposition following screen printing TiO_2 film electrode in 0.1 M KCl solution containing 2.5 mM $Fe(CN)_6^{3-/4-}$ at an open circum potential. **b** An equivalent circuit $R_s(R_{ct}CPE)W_o$ used to model the impedance data
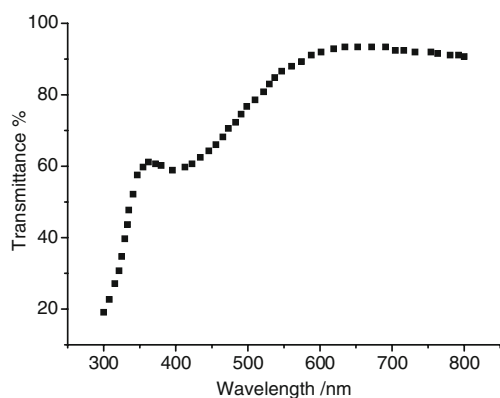
Fig. 5 The transmittance spectra of the close-packed TiO_2 film on ITO substrate by electrodeposition at 0.1 V for 20 min. Bare ITO used as reference

related photocurrent density, donated as R_{JSC}, was calculated by the following formula:

$$R_{JSC} = J_{SC, tTiO_2/ITO} / J_{SC, sTiO_2/ITO}$$

Where $J_{SC,tTiO_2/ITO}$ is the photocurrent density of tTiO₂/ITO measured in the corresponding DSSC and $J_{SC,sTiO_2/ITO}$ the photocurrent density of sTiO₂/ITO without the under-layered close-packed TiO_2 film. The related photocurrent density increased as the thickness of the deposited TiO_2
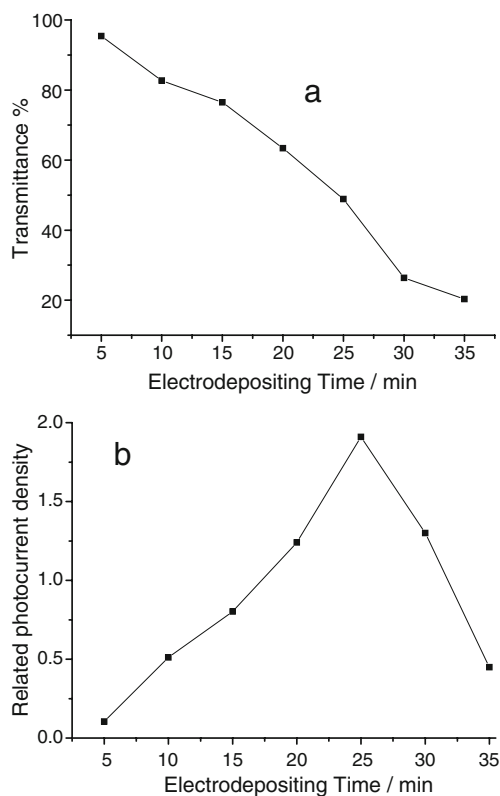
compact layer increased and reached a maximum at the electrodepositing time, 25 min. It was reported that the increase in photocurrent density was mainly due to the effective inhibition of recombination of charges, which led to more electrons injecting from dye to the ITO anode, via the mesoporous TiO_2 and close-packed TiO_2 blocking film [19]. The thicker the close-packed TiO_2 films, the more effective they block the holes produced from getting through to the anode and, therefore, resulting in an increase in photocurrent density. By further increasing the film thickness, however, the related photocurrent density decreased. The much thicker close-packed TiO_2 (e.g., electrodepositing time, 35 min, and the thickness, 460 nm) could hinder the desired number of electrons reaching the ITO anode due to its surface defaults and poor light transmittance as discussed above [19]. Therefore, an optimum thickness, 400 nm, of the blocking TiO_2 layer, corresponding to electrodepositing time, 25 min, was appreciated to balance the blocking of dark current recombination and transportation of electrons.

At the optimum thickness of 400 nm, the photovoltage (V_{OC}), photocurrent density (J_{SC}), and the fill factor (FF) of tTiO₂/ITO-based cell were 0.416 V, 1.19 mA/cm², and 0.46, respectively (Fig. 7). According to these results, it was concluded that the performance was better than that of sTiO₂/ITO-based cell (0.363 V, 0.585 mA/cm², and 0.49). In other words, the close-packed TiO_2 layer was effective to reduce the dark current, thereby to improve the performance of DSSC.

Conclusions

A uniform, tight, and close-packed TiO_2 nanocrystalline film on the ITO substrate was fabricated by an electro-depositing method. This compact layer could effectively inhibit the recombination of charges and led to more electrons injecting from dye through the mesoporous TiO_2
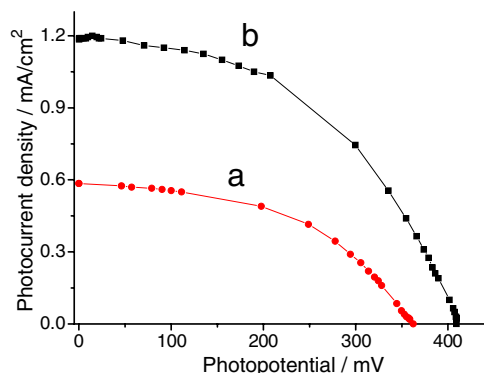

Fig. 6 a The effect of electrodeposition time on transmittance of the close-packed TiO_2 film at 358 nm using bare ITO as a reference. **b** Plots of related photocurrent density vs. electrodeposition times

Fig. 7 Photoelectric characterization of a ZnPcTc-sensitized TiO_2 film solar cell with **a** sTiO₂/ITO, **b** tTiO₂/ITO (0.1 V, 25 min)

and close-packed TiO_2 blocking film to the ITO anode, and therefore improved the performances of the corresponding cells. The effects of film thickness on light transmittance and photocurrent density of the corresponding cell were also demonstrated. Considering the largest related photocurrent density and good light transmittance, the optimum film thickness was found to be approximately 400 nm. Using this optimum thickness film, the photocurrent density greatly increased comparing with that of the screen printing TiO_2 film. The improvements of the photoelectrical characteristics made the proposed method potential to be used for practical fabrication of DSSC.

References

1. O'Regan B, Grätzel M (1991) Nat 353:737. doi:10.1038/353737a0
2. Grätzel M (2003) J Photochem Photobiol Chem 4:145. doi:10.1016/S1389-5567(03)00026-1
3. Wang ZS, Kawauchi H, Kashima T, Arakawa H (2004) Coord Chem Rev 248:1381. doi:10.1016/j.ccr.2004.03.006
4. He JJ, Benkö G, Korodi F, Polívka T, Lomoth R, Åkermark B, Sun LC, Hagfeld A, Sundström V (2002) J Am Chem Soc 124:4922. doi:10.1021/ja0178012
5. Cameron PJ, Peter LM (2003) J Phys Chem B 107:14394. doi:10.1021/jp030790+
6. Yum J-H, Kim S-S, Kim D-Y, Sung Y-E (2005) J Photochem Photobiol A 173:1. doi:10.1016/j.jphotochem.2004.12.023
7. Ito S, Liska P, Comte P, Charvet R, Péchy P, Bach U, Schmidt-Mende L, Zakeeruddin SM, Kay A, Nazeeruddin MK, Grätzel M (2005) Chem Commun (Camb) 5:4351. doi:10.1039/b505718c
8. Peng B, Jungmanna G, Jäger C, Haarer D, Schmidt HW, Thelakkat M (2004) Coord Chem Rev 248:1479. doi:10.1016/j.ccr.2004.02.008
9. Hart JN, Menzies D, Cheng YB, Simon GP, Spiccia L (2006) C R Chim 9:622
10. Zhu K, Schiff EA, Park NG, van de Lagemaat J, Frank AJ (2002) Appl Phys Lett 80:685. doi:10.1063/1.1436533
11. Acher BN, Fohlen GM, Parker JA, Keshavayya J (1988) Indian J Chem Sect A 27:411
12. Bisquert J (2002) J Phys Chem B 106:325. doi:10.1021/jp011941g
13. Kern R, Sastrawan R, Ferber J, Stangl R, Luther J (2002) Electrochim Acta 47:4213. doi:10.1016/S0013-4686(02)00444-9
14. Adachi M, Sakamoto M, Jiu J, Ogata Y, Isoda S (2006) J Phys Chem B 110:13872. doi:10.1021/jp061693u
15. Zhang JJ, Wu M, Qin YT, Chen R, Jiang YH, Sun YM, Yang ZH (2008) Acta Phys Chim Sin 24:79
16. Bard AJ, Faulkner LR (1980) Electrochemical methods: fundamentals and applications. Wiley, New York
17. Stoynov ZB, Grafov BM, Savova-Stoynova BS, Elkin VV (1991) Electrochemical impedance. Nauka, Moscow
18. Chen A, La Russa DJ, Miller B (2004) Langmuir 20:9695. doi:10.1021/la0484873
19. Cameron PJ, Peter LM, Hore S (2005) J Phys Chem B 109:930. doi:10.1021/jp0405759